Propagation of a Shock Wave

Amir Baharvand

The problem of propagation of a shock wave is given in [1]. In the present solution, we discuss problems 7.3 to 7.4 of the same book.

1 Displacement, Problem 7.3

The displacement, u, due to propagation of a shock wave in a cavity in an infinite medium is

$$u = \frac{pa^3}{4\mu r^2}\left\{1 - \left(\cos\theta - \frac{2r-a}{\alpha a}\sin\theta\right)e^{-\frac{c_p\tau}{2da}}\right\}H(\tau) \tag{1}$$

where

$$\alpha = \frac{1}{\sqrt{1-2\nu}} \quad ,\tau = t - \frac{r-a}{c_p} \quad ,d = \frac{1-\nu}{2-4\nu} \quad ,\theta = \frac{\alpha c_p \tau}{2da}$$

$$c_p = \sqrt{\frac{\lambda+2\mu}{\rho}} \quad ,\lambda = \frac{E\nu}{(1+\nu)(1-2\nu)} \quad ,\mu = \frac{E}{2(1+\nu)} \tag{2}$$

p is the pressure, a is the cavity radius, r is the radial distance, ν is the Poisson's ratio, t is time, c_p is the wave propagation speed, E is the Young's modulus, ρ is density, λ and μ are Lame's constants and H is the Heaviside function.

The displacement on the boundary of the cavity ($r = a$) then reduces to

$$u_0 = \frac{pa}{4\mu}\left\{1 - \left[\cos\left(\frac{\alpha c_p t}{2da}\right) - \frac{1}{\alpha}\sin\left(\frac{\alpha c_p t}{2da}\right)\right]e^{-\frac{c_p t}{2da}}\right\}H(t) \tag{3}$$

Figure. 1a shows the displacement on the cavity boundary, u_0, for various Poisson's ratios. The time axis is normalized by $\frac{c_p}{a}$ where c_p is determined from Eq. 2. t can also be normalized by another parameter, $\frac{c_1}{a}$ where $c_1 = \sqrt{\frac{E}{\rho}}$ which is shown in Figure. 1b.

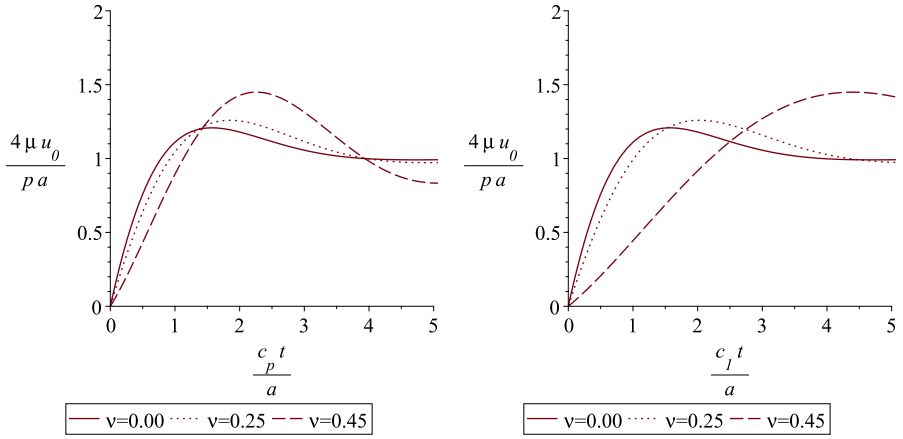

(a) Normalized t using c_p.

(b) Normalized t using c_1.

Figure 1: Normalized displacement on the cavity boundary ($r = a$).

One may notice that while c_p is dependent on the Poisson's ratio (see Eq. 2), c_1 is not, which justifies different periods of plots for various ν in Figure. 1. The period, T, of plots in Figure. 1 are summarized and compared in Table. 1.

i	ν	T_{c_p}	$\frac{T_{c_p,(i+1)}}{T_{c_p,i}}$	T_{c_1}	$\frac{T_{c_1,(i+1)}}{T_{c_1,i}}$
1	0	1.51	-	6.38	-
2	0.25	1.49	0.97	6.73	1.05
3	0.45	5.69	3.82	10.96	1.62

Table 1: Periods of plots in Figure. 1 for E=1 and ρ=1.

It is evident from the fourth and sixth columns of Table. 1 that the periods of plots for different ν get closer if we normalize the time axis by $\frac{c_1}{a}$.

2 Determination of the Stress Wave Traveling Time, Problem 7.4

For this problem, the radial stress, σ_r, from Eq. 4 is plotted for a cavity of radius $a = 1$m in soil with a wave propagation speed, $c_p = 1000$m/s.

$$\sigma_r = -\frac{pa^3}{r^3}\left\{1 + \left(\frac{r^2 - a^2}{a^2}\cos\theta - \frac{1}{\alpha}\left(\frac{r-a}{a}\right)^2 \sin\theta\right) e^{-\frac{c_p \tau}{2da}}\right\} H(\tau) \qquad (4)$$

α, τ, d and θ can be found from Eq. 2. Figure. 2 provides a visualisation of σ_r for three cases of ν at different distance, r, from the cavity. It is

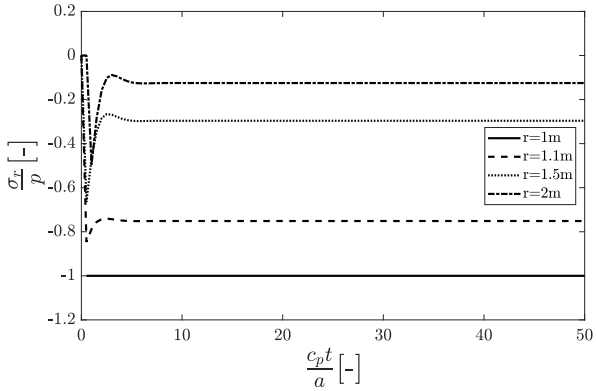

(a) $\nu = 0$

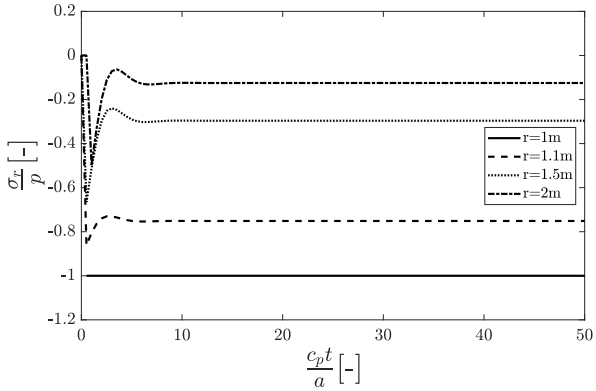

(b) $\nu = 0.25$

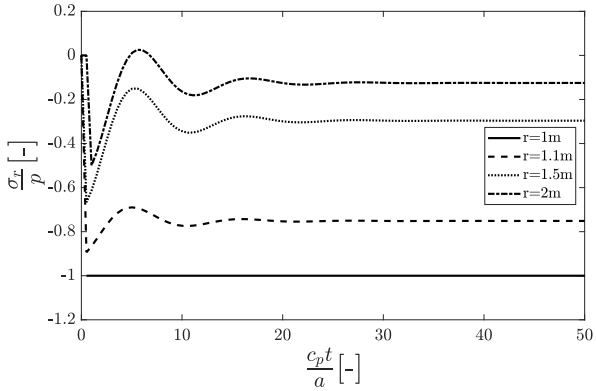

(c) $\nu = 0.45$

Figure 2: Normalized radial stress for various values of ν at different distances, r, from the cavity.

clearly visible that by increasing the Poisson's ratio, the required time to reach stability rises. For instance, for the case $\nu = 0$, at $r = 2$m, σ_r stabilizes at about $\frac{c_p t}{a}$ =7.5, while the stability time for the same distance for $\nu = 0.25$ and $\nu = 0.45$ are 11 and 28, respectively. It is worth noting that the initial value of σ_r is zero for the very first values of time and this mounts by increasing the radius. The reason behind this phenomenon is the wave propagation speed, as it takes some time for a point at distance to realize the generated stress wave.

By plotting the variation of Poisson's ratio for the range $0 \leq \nu \leq 0.45$ versus the stability time (Figure. 3) for $r = 4a$, it is seen that the stability time monotonically rises by increasing ν. It is worth mentioning that the relative error of less than 1% for the value of radial stress is taken as the stability time criterion.

The stability time, in all the cases in Figure. 2, decreases by moving further away from the cavity as a result of the damping coefficient (the exponential term in Eq. 4). This falling behavior of stability time versus radius is plotted in Figure. 4. The first point in Figure. 4 has the lowest value as in this case $r = a$; thus, the damping coefficient vanishes. The stability time criterion is chosen as the former case (the effect of Poisson's ratio on the stability time).

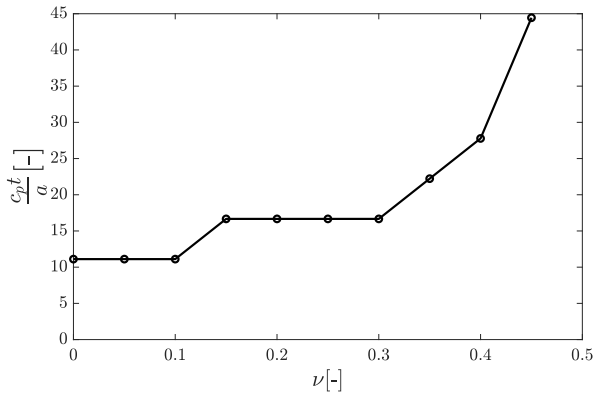

Figure 3: The effect of Poisson's ration on stability time ($0 \leq \nu \leq 0.45$ at $r = 4a$).

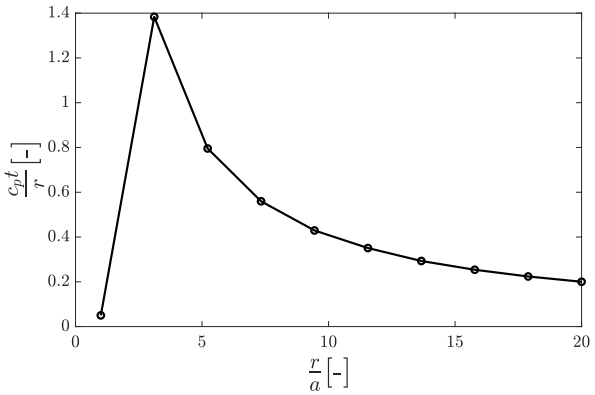

Figure 4: The effect of distance from the cavity on stability time ($a \leq r \leq 20a$ at $\nu = 0.45$).

3 Determination of the Stress at Infinity, Problem 7.5

Rewriting Eq. 4 and taking the limit when $\frac{r}{a} \to \infty$ results in zero stress which indeed coincides the radiation boundary condition ($\sigma_r = 0$ when $r \to \infty$ for $t > 0$). This vanishing point at infinite distance from the cavity for three cases of ν is also shown in Figure. 5

$$\lim_{\frac{r}{a} \to \infty} -\frac{pa^3}{r^3} \left\{ 1 + \left(\left[\left(\frac{r}{a} \right)^2 - 1 \right] \cos\theta - \frac{1}{\alpha} \left(\frac{r}{a} - 1 \right)^2 \sin\theta \right) e^{-\frac{c_p \tau}{2da}} \right\} H(\tau) = 0$$

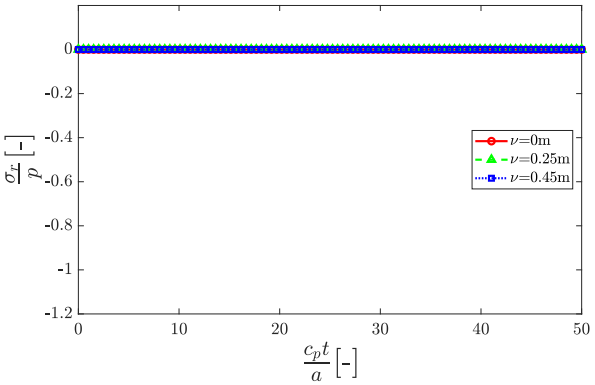

Figure 5: Normalized radial stress for various Poisson's ratios for $\frac{r}{a} \gg 1$.

References

[1] A. Verruijt, *An Introduction to Soil Dynamics*. Theory and Applications of Transport in Porous Media, Springer Netherlands, 1st edition ed., 2010.